Properties of jet engine combustion particles during the PartEmis experiment. Hygroscopic growth at supersaturated conditions

R. Hitzenberger,[1] H. Giebl,[1] A. Petzold,[2] M. Gysel,[3] S. Nyeki,[3] E. Weingartner,[3] U. Baltensperger,[3] and C. W. Wilson[4]

Received 11 March 2003; revised 19 May 2003; accepted 10 June 2003; published 31 July 2003.

[1] During the EU Project PartEmis, the microphysical properties of aircraft combustion aerosol were investigated. This study is focused on the ability of exhaust aerosols to act as cloud condensation nuclei (CCN). The combustor was operated at two different conditions representing old and modern aircraft engine technology. CCN concentrations were measured with the University of Vienna CCN counter [*Giebl et al.*, 2002] at supersaturations around 0.7%. The activation ratio (fraction of CCN in total aerosol) depended on the fuel sulphur content (FSC) and also on the operation conditions. CCN/CN ratios increased from 0.93 through 1.43 to $5.15 \cdot 10^{-3}$ (old cruise conditions) and 0.67 through 3.04 to $7.94 \cdot 10^{-3}$ (modern cruise conditions) when FSC increased from 50 through 410 to1270 μg/g. The activation behaviour was modelled using classical theories and with a semi-empirical model [*Gysel et al.*, 2003] based on measured hygroscopicity of the aerosol under subsaturated conditions, which gave the best agreement. *INDEX TERMS:* 0305 Atmospheric Composition and Structure: Aerosols and particles (0345, 4801); 0320 Atmospheric Composition and Structure: Cloud physics and chemistry; 0345 Atmospheric Composition and Structure: Pollution—urban and regional (0305). **Citation:** Hitzenberger, R., H. Giebl, A. Petzold, M. Gysel, S. Nyeki, E. Weingartner, U. Baltensperger, and C. W. Wilson, Properties of jet engine combustion particles during the PartEmis experiment. Hygroscopic growth at supersaturated conditions, *Geophys. Res. Lett.*, *30*(14), 1779, doi:10.1029/2003GL017294, 2003.

1. Introduction

[2] Emissions of particles by aircraft contribute to the aerosol in the upper troposphere and lowermost stratosphere (UTLS) and are currently under intense investigation [*IPCC*, 2001]. Insoluble carbonaceous particles emitted from aircraft engines play an important role in contrail formation [*Kärcher*, 1999] and have a high potential to initiate cirrus cloud formation via heterogeneous freezing processes. They require saturation ratios close to unity with respect to liquid water at typical UTLS temperatures for ice nuclei (IN) activation. A coating with H_2SO_4 reduces the critical saturation ratio considerably [*DeMott et al.*, 1997].

[3] Previous laboratory studies investigated the activation ratio R_{act} (defined as the number fraction of CCN) in combustion aerosols at liquid water supersaturations $\leq$1%. Reported values of the R_{act} vary from 0.008 [*Hudson et al.*, 1991] to 0.3 [*Whitefield et al.*, 1993]. In situ measurements in aircraft plumes yielded R_{act} from $\leq$0.01 [*Pitchford et al.*, 1991] to 0.5 [*Hudson and Xie*, 1998] at a supersaturation of 0.8–1.0%. Comparable measurements for IN activation are not available. A maximum IN-R_{act} of about 0.2 was estimated from near field measurements in an aircraft plume [*Petzold et al.*, 1997].

[4] In the framework of the PartEmis project (Wilson et al., Measurement and prediction of emissions of aerosols and gaseous precursors from gas turbine engines (PartEmis): an experimental overview, submitted to *Aerospace Science and Technology*, 2003, hereinafter referred to as Wilson et al., submitted manuscript, 2003) the effect of operation conditions and fuel sulphur content (FSC) on the microphysical and chemical properties of the emitted particles was investigated. This paper will focus on the CCN activation of combustion aerosol particles. Microphysical and chemical properties [*Petzold et al.*, 2003] and the hydration properties at water subsaturated conditions [*Gysel et al.*, 2003] are investigated elsewhere.

2. Experimental Methods

[5] The combustor of the QinetiQ TRACE engine (Wilson et al., submitted manuscript, 2003) was operated at two conditions with different inlet temperatures representing the gas path temperatures of older (T = 566K, ''old operating conditions'') and more modern (T = 766K, ''modern operating conditions'') jet engines. Fuels with three different sulphur contents (FSC; 50, 410 and 1270 μg g^{-1}) were used. A sampling probe was moved stepwise with 11 different positions through the combustor exit plane. Each sampling condition (probe position, FSC and operation condition) was assigned a test point number. The exhaust gas was cooled immediately to 150°C. Part of this cooled exhaust was diluted ca. 70 ms after entering the sampling probe by a factor of about 65 using pre-filtered ambient air which resulted in a sample temperature between 20 and 25°C, relative humidity $\leq$10% and pressure of 1020–1050 hPa). All instruments providing data for this study were sampling from the diluted line. The travel time of the aerosol between the sampling ports of the CN and humidity and volatility DMAs and the CCN counter was ca. 0.2 sec. Because of the high dilution and large line diameter (21.2 mm), no appreciable losses of particles are expected between the sampling ports, so the data should be comparable.

[6] The CCN concentration was measured at supersaturations S between 0.53 and 0.75% in the diluted sample stream

[1]Institute for Experimental Physics, University of Vienna, Vienna, Austria.
[2]DLR, Institut für Physik der Atmosphäre, Oberpfaffenhofen, Germany.
[3]Paul Scherrer Institut, Villigen, Switzerland.
[4]QinetiQ, Farnborough, UK.

0094-8276/03/2003GL017294$05.00

with the University of Vienna cloud condensation nuclei counter (CCNC-UniV [*Giebl et al.*, 2002]), which is based on a static thermal diffusion chamber. CCN that can be activated at the selected S grow to large (>10 μm) droplets which are illuminated by a laser beam, photographed with a CCD camera (sampling frequency of 15/sec) and counted on-line. The counting efficiency was 1.0 ± 0.09.

3. Theoretical Models

3.1. Classical Models (Köhler, Kelvin, Coated Sphere)

[7] CCN are a subset of the atmospheric aerosol and are defined as particles that undergo (theoretically) unlimited growth when exposed to a water vapour supersaturation equal to or larger than a specified S in a CCN counter. The equilibrium size of soluble particles is described by Köhler theory, while Kelvin theory describes the equilibrium diameter for insoluble but wettable particles [e.g., *Pruppacher and Klett*, 1997]. In this paper, we used the equations given by *Giebl et al.* [2002] to calculate the activation diameters of soluble and insoluble particles for the S set in the CCNC. As the predominantly insoluble combustion particles are known to contain also some volatile, semivolatile, and water soluble material, we used also a modified Köhler equation for a particle with an insoluble core and a coating of a soluble substance (coated sphere model) [*Pruppacher and Klett*, 1997]. Volatility measurements [*Petzold et al.*, 2003] gave volatile mass fractions of 1, 3 and 5% for low, mid and high FSC in the size range of CCN.

[8] All the models described in this section assume spherical particles or aqueous solution droplets containing only a single solute with well defined physico-chemical properties. In the case of our measurements, neither the full chemical composition of the material nor the variation in chemical composition of particles in a narrow size class are known, so we assumed the volatile and/or soluble material to be H_2SO_4.

3.2. HTDMA Model

[9] The humidity growth of the combustion aerosol was investigated under subsaturated conditions [*Gysel et al.*, 2003] with a hygroscopicity tandem differential mobility analyser (H-TDMA) for size fractions 30, 50 and 100 nm. Experimental growth factors were fitted by a semi-empirical model (HTDMA model), assuming an insoluble core with a H_2SO_4 shell of variable thickness. Potential restructuring of the core was also included. Estimates of the volume fraction ε of H_2SO_4 showed a marked decrease of ε for increasing particle size. The ε were similar to or smaller than the volatile fractions (e.g. for particles of D = 100 nm, ε = 0.2, 1.2, and 3% for modern cruise conditions and low, medium, and high FSC) in the size range of measured activation diameters. Extrapolation of modelled growth curves to supersaturated conditions yielded size dependent critical S values, which were used to estimate CCN concentrations (details in *Gysel et al.* [2003]). Error bars in Figure 3 indicate the sensitivity of CCN estimates to lower and upper limits of HTDMA model parameters.

4. Results

4.1. Measured and Modelled CCN Activation

[10] CCN concentrations were measured at each test point. At the beginning of the measurement period, S was unstable because of technical reasons. The first five data points for old cruise conditions and low FSC are therefore not considered in the discussion of CCN properties. As expected, the CCN concentration increased with increasing FSC (see Figure 3 below, concentrations multiplied by the dilution ratio for comparability with other studies). The most interesting parameters for activation studies, however, are the activation ratio R_{act} and the apparent activation diameter, which is the minimum diameter of a dry combustion particle that may be activated as a CCN at a certain supersaturation.

Table 1. Average Values (Top Lines) and Standard Deviations (Next Lines) Over All Test Points Within One Set of Measurements of Apparent Activation Diameters (CCN-D). Predicted Activation Diameters for all models (Kelvin-D, Köhler-D, Coated-D, and HTDMA-D

Test Condition	OL	OM	OH	ML	MM	MH
CCN D, nm	244.3	200.3	146.9	301.1	179.6	145.6
	13.4	18.4	16.7	43.5	13.4	11.2
Kelvin D, nm	301.5	295.7	290.3	324.3	315.7	288.5
	10.5	2.4	3.5	11.7	7.2	6.0
Koehler D, nm	30.5	30.1	29.7	32.0	31.4	29.6
	0.7	0.2	0.2	0.8	0.5	0.3
Coated D[a] nm	130	94	79	137	99	79
	8	0	0	4	0	0
HTDMA D, nm	277	208	94	292	157	93
CMD, nm	40.6	39.5	36.9	43.7	40.1	40.1
	2.6	4.8	4.8	1.9	3.3	2.8
CCN activation ratio $*10^{-3}$	1.00	1.43	5.15	0.67	3.04	7.94
	0.34	0.51	0.72	0.19	0.80	3.83

The count median diameters (CMD) of the number size distributions and the activation ratios (fractions of CCN-activated particles relative to the total particle concentration) are also given.

[a]Volatile fractions 1, 3, and 5% for low, medium and high FSC.

[11] During PartEmis, the total CN concentration (d 10 nm) was measured with CN counters [*Petzold et al.*, 2003] and the number size distribution was measured with an SMPS system (Scanning Mobility Particle Spectrometer, [Wilson et al., submitted manuscript, 2003] for all test points and fitted with lognormal functions. In general, the shape of all measured distributions was found to be rather similar. Both the average value over all probe positions and the standard deviation of the count median diameter (CMD, see Table 1) of these fitted distributions depended only very weakly on operation conditions or FSC. At the large particle end, however, where concentrations are very low, the measured data points scattered widely. As potential CCN have sizes in this range, the measured distributions were used rather than the fitted lognormal ones to calculate R_{act} and the apparent activation diameter.

[12] As a first step, an apparent activation diameter (CCN-D) was obtained from the measured size distributions as the lower cut size leading to number concentrations equal to the measured CCN concentrations. CCN-D decrease from 237 and 301 nm at low FSC to 147 and 146 nm at high FSC for old and modern cruise conditions, respectively. Activation diameters were also calculated for all models. Table 1 shows these diameters as averages over all probe positions for each operation condition and all models, while Figure 1 gives the values for all the test points.

[13] The Köhler model (H_2SO_4 particles) predicts critical diameters that are distinctly (80% to 90%) smaller than

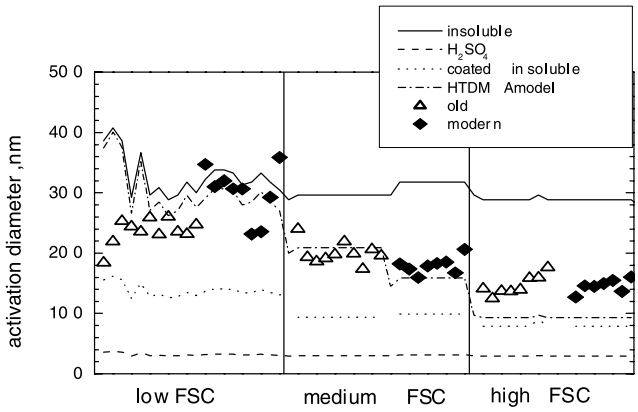

Figure 1. Apparent activation diameter for old and modern conditions (open triangles and solid diamonds, resp.); theoretical values for the Kelvin (insoluble), Köhler (H_2SO_4), coated sphere (coated insoluble) and HTDMA model are added as lines. X values are test point numbers.

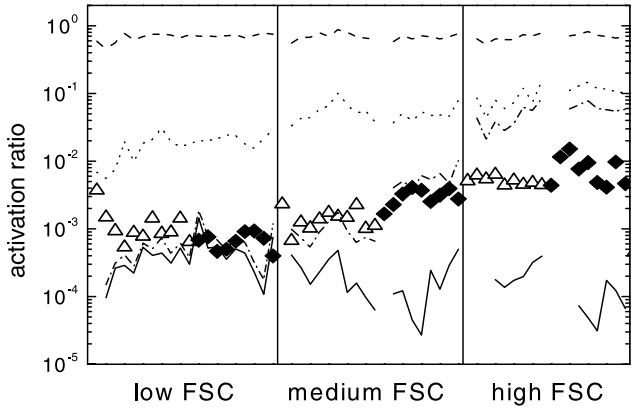

Figure 2. Fraction of CCN-activated combustion aerosol particles ($\geq$10 nm) at a supersaturation of 0.7%; values are given for old (open triangles) and modern (solid diamonds) conditions, lines refer to predictions of the Köhler (solid) and Kelvin (dashed), coated sphere (dotted) and HTDMA model (dashed-dotted). X values are test point numbers.

measured CCN-D which is expected because large combustion particles are not completely water soluble. The assumption of completely insoluble particles (Kelvin model) provides the largest critical diameters. Kelvin-D are 26 and 8% at low FSC and 98 and 98% at high FSC larger than CCN-D under old and modern conditions. This indicates that the soluble fraction of the particles increases from low FSC to high FSC level. The coated sphere model (Coated-D) underestimates critical diameters by 45 to 55% under all conditions. The HTDMA model (HTDMA-D) provides the best predictions of CCN-D. HTDMA-D agrees within ±16% with CCN-D at low and medium FSC. At high FSC HTDMA-D are 36% smaller than CCN-D.

[14] The effect of cruise conditions on the CCN-D is unclear (see Table 1 and Figure 1). Differences between old and modern cruise conditions are +26, −10, and −1% at low, medium and high FSC. Similar trends were observed for hygroscopic properties under subsaturated conditions [*Gysel et al.*, 2003], which is reflected by differences of predicted HTDMA-D between old and modern cruise conditions of +5.4, −25, and −1% for low, medium and high FSC.

[15] The ratio (R_{act}) of measured CCN concentrations to the total number concentrations of particles $\geq$10 nm was calculated for all conditions. For modeling R_{act}, estimated CCN concentrations obtained by summing the size distributions using the activation diameters as lower cut size were used. Figure 2 shows measured as well as the modelled R_{act} for all test points. The measured R_{act} at low FSC are near the Kelvin R_{act} and increase with increasing FSC without reaching R_{act} calculated with the coated sphere model.

[16] Compared to typical ambient atmospheric aerosols, where CCN/CN ratios are of the order of 0.2 to 0.6 for maritime air and 0.004 to 0.02 for continental air [*Pruppacher and Klett*, 1997], measured R_{act} in the combustor exhaust is low with values around 0.001 at low and mid FSC and 0.01 at high FSC (see Table 1). The values are within the range given in the literature (see Introduction) for combustion and aircraft aerosol, but significantly lower than 0.3 as found by *Whitefield et al.* [1993] for ca. 1000 ppm FSC and 0.5 [*Hudson and Xie*, 1998]. Part of this difference could be due to different S (the high literature values were obtained for S = 0.8−1%) or FSC (not always reported).

4.2. Estimated CCN Concentrations

[17] As an example, estimated CCN concentrations are shown in Figure 3 for modern cruise conditions (all FSC). For low FSC the activation of the particles seems to follow Kelvin theory, while the increased H_2SO_4 content under mid and high FSC results in an enhanced activation. For low FSC, both Kelvin activation and the HTDMA model reproduce the measured CCN concentrations best. For mid and high FSC the measured concentrations are best reproduced by the HTDMA model, which overestimates the CCN concentrations under modern cruise conditions only by factors of about 2 and 7. For old cruise conditions, the

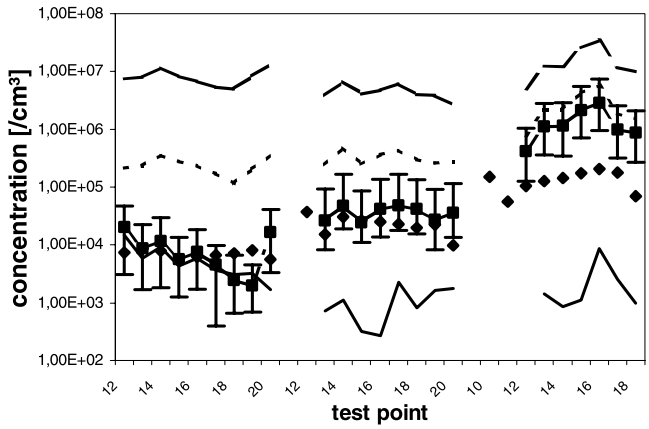

Figure 3. Measured CCN concentrations (diamonds) compared to CCN concentrations estimated from the models for modern cruise conditions and low (left), medium (centre) and high FSC (right). The error bars correspond to the maximum and minimum CCN concentrations estimated from the HTDMA model. Full lines: Kelvin, squares: HTDMA, dotted: coated sphere. Topmost line: Köhler model.

modelled CCN concentrations are 0.5 and 0.7 (low and mid FSC) and 8 (high FSC) times the measured concentrations.

5. Discussion

[18] The measured R_{act} and activation diameters depend on the FSC. CCN-D decreases with increasing fuel sulphur content. These findings agree well with the hygroscopic behaviour at subsaturated conditions [*Gysel et al.*, 2003]. All calculated activation diameters are in the size range (ca. 30–300 nm) where the aerosol was found to be completely internally mixed with respect to volatile and semivolatile material [*Petzold et al.*, 2003] as well as to their hygroscopic behaviour [*Gysel et al.*, 2003].

[19] Regarding all FSC, the coated sphere model reproduces CCN-D best among the classical models, but predicted values are 45 to 55% smaller. In the case of R_{act}, the Kelvin model gives the best fit among the classical models under low FSC and also at medium FSC and old cruise conditions. On the other hand, the HTDMA model, which uses parameters measured under subsaturated conditions, gives the best fit to the measured data under all conditions.

[20] Several interpretations of these findings are possible. Calculations of the activation diameter of spherical particles coated with 1% H_2SO_4 showed that the thickness of the shell would be only 0.43 and 0.46 nm (for old and modern conditions), which is insufficient for coating the insoluble core with a monolayer of H_2SO_4 molecules. At medium and high FSC, the layer thickness is 1 nm and 1.3 nm. In both these cases, contiguous H_2SO_4 layers are theoretically possible. If the soluble material is not distributed evenly among all particles in the size range of possible CCN, only the particles with the largest fractions of this material will be activated. The combustion particles collected at 150°C contain about 30% OC by mass [*Petzold et al.*, 2003]. Some of this OC could be water soluble and/or surface active or could form a surface film that might inhibit water uptake to some extent. The presence of soluble material other than H_2SO_4 will influence the activation behaviour of combustion particles, but the available information is insufficient to predict this influence.

6. Summary and Conclusions

[21] In the combustion aerosol, measured CCN (at ≈0.7% supersaturation) activation ratios R_{act} depended on FSC. An increase of FSC by a factor of 25 resulted in an increase of the R_{act} by a factor of 12. The R_{act} determined in this experiment are 0.001 and 0.008 at low and high FSC,, which is low compared to literature values. Except for the low FSC case, the more modern operation conditions produced R_{act} that were nearly twice as high as those for the old conditions. Apparent activation diameters were found to decrease from 236.6 and 301.1 nm at low FSC to 146.9 and 145.6 nm at high FSC for old and modern conditions. The Köhler model (soluble particles) cannot reproduce measured activation properties. The Kelvin model (insoluble but wettable particles) provides good predictions for low FSC, but activation diameters (ratios) are increasingly overestimated (underestimated) at medium and high FSC. This indicates that the soluble fraction of the combustion particles increases from low values at low FSC level to relatively large values at high FSC. The coated sphere model, which equates the measured volatile fraction with soluble H_2SO_4, underestimates the activation diameter by 45 to 55% under all conditions. A small amount of semivolatile organics with low or absent water-solubility adsorbed on the combustion particles might be one reason for this discrepancy. The HTDMA model, which also assumes that the hygroscopic material is H_2SO_4, but estimates CCN concentrations using parameters obtained from the hygroscopicity measurements, gives the best fit to the measured data for all FSC levels.

[22] **Acknowledgments.** The PartEmis project is funded by the European Commission (G4RD-CT-2000-00207) and the Swiss Bundesamt für Bildung und Wissenschaft (99.0632). The test rig operation crew at QinetiQ gave invaluable support during the experiments. The development of the CCNC was funded by the Austrian Science Fund (FWF; P10328-CHE and P13143-CHE).

References

DeMott, P. J., D. C. Rogers, and S. M. Kreidenweis, The susceptibility of ice formation in upper tropospheric clouds to insoluble aerosol components, *J. Geophys. Res.*, *102*, 19,575–19,584, 1997.

Giebl, H., et al., CCN activation of oxalic and malonic acid test aerosols with the Univ. of Vienna cloud condensation nuclei counter, *J. Aerosol Sci.*, *33*, 1623–1634, 2002.

Gysel, M., et al., Properties of jet engine combustion particles during the PartEmis experiment: Hygroscopicity at subsaturated conditions, *Geophys. Res. Lett.*, *30*(11), 1566, doi:10.1029/2003GL016896, 2003.

Hudson, J. G., J. Hallett, and C. F. Rogers, Field and laboratory measurements of cloud-forming properties of combustion aerosols, *J. Geophys. Res.*, *96*, 10,847–10,859, 1991.

Hudson, J. G., and Y. Xie, Cloud condensation nuclei measurements in the high troposphere and in jet aircraft exhaust, *Geophys. Res. Lett.*, *25*, 1395–1398, 1998.

IPCC, et al., Climate Change 2001: The Scientific Basis, Cambridge Univ. Press, Cambridge, UK, 2001.

Kärcher, B., Aviation-produced aerosols and contrails, *Surv. Geophys.*, *20*, 113–167, 1999.

Petzold, A., et al., Near field measurements on contrail properties from fuels with different sulfur content, *J. Geophys. Res.*, *102*, 29,867–29,880, 1997.

Petzold, A., et al., Properties of jet engine combustion particles during the PartEmis experiment: Microphysical and chemical properties, *Geophys. Res. Lett.*, *30*(13), doi:10.1029/2003GL017283, 2003.

Pitchford, M., et al., Size and critical supersaturation for condensation of jet engine exhaust particles, *J. Geophys. Res.*, *96*, 20,787–20,793, 1991.

Pruppacher, H. R., and J. D. Klett, Microphysics of Clouds and Precipitation. 2nd edition, Kluwer, Dordrecht, 1997.

Whitefield, P. D., M. B. Trueblood, and D. E. Hagen, Size and hydration characteristics of laboratory simulated jet engine combustion aerosols, *Particul. Sci. and Technol.*, *11*, 25–36, 1993.

H. Giebl and R. Hitzenberger, Institute for Experimental Physics, University of Vienna, Vienna, Austria.

A. Petzold, DLR, Institut für Physik der Atmosphäre, Oberpfaffenhofen, Germany.

U. Baltensperger, M. Gysel, S. Nyeki, and E. Weingartner, Paul Scherrer Institut, Laboratory of Atmospheric Chemistry, Villigen, Switzerland.

C. W. Wilson, QinetiQ, Farnborough, UK.